Semicond. Sci. Technol. 23 (2008) 105015 (6pp) doi:10.1088/0268-1242/23/10/105015

Investigation of responsivity decreasing with rising bias voltage in a GaN Schottky barrier photodetector

Shuang Zhang, D G Zhao[1], D S Jiang, W B Liu, L H Duan, Y T Wang, J J Zhu, Z S Liu, S M Zhang and Hui Yang

State Key Laboratory on Integrated Optoelectronics, Institute of Semiconductors, Chinese Academy of Sciences, PO Box 912, Beijing 100083, People's Republic of China

E-mail: dgzhao@red.semi.ac.cn

Received 29 January 2008, in final form 10 August 2008
Published 9 September 2008
Online at stacks.iop.org/SST/23/105015

Abstract

The unexpected decrease in measured responsivity observed in a specific GaN Schottky barrier photodetector (PD) at high reverse bias voltage was investigated and explained. Device equivalent transforms and small signal analysis were performed to analyse the test circuit. On this basis, a model was built which explained the responsivity decrease quantitatively. After being revised by this model, responsivity curves varying with bias voltage turned out to be reasonable. It is proved that the decrease is related to the dynamic parallel resistance of the photodiode. The results indicate that with a GaN Schottky PD, the choice of load resistance is restricted according to the dynamic parallel resistance of the device to avoid responsivity decay at high bias voltage.

(Some figures in this article are in colour only in the electronic version)

1. Introduction

In recent years, an increasing number of works have been done focused on the detection of UV radiation. High-quality UV detectors are required for applications in many fields, such as flame sensors, engine control, missile plume detection, UV astronomy and secure space-to-space communications [1]. Group III-nitride materials (AlN, GaN and their ternary compounds) provide a superior candidate for the fabrication of high-efficiency UV detectors because of their wide band gap tunable from 3.42 eV (GaN) to 6.2 eV (AlN) according to different Al components, leading to a cutoff wavelength of a photodetector (PD) ranging from 200 nm to 360 nm and good rejection at a longer wavelength [2]. Different structures of UV detectors have been reported based on III-nitride materials, such as photoconductive detectors [3], p–n junction PDs [4], p–i–n PDs [5, 6], Schottky barrier PDs [7] and metal–semiconductor–metal (MSM) PDs [8–10]. The development of III-nitride PDs promotes the fabrication of a UV focus plane array (FPA) camera which can provide UV detection images [11, 12]. In a FPA camera, the PD array is connected to a readout integrated circuit (ROIC) with the bonding technique, so that the photo-generated signal can be collected and output by the ROIC. The characteristics of devices and the parameters of the ROIC interact with each other. So it is very important to choose the type and parameters of the readout circuit according to the characteristics of the detector, such as static work point, dark current level, dynamic parallel range of the detector, etc, for the satisfactory performance of the UV FPA camera [13].

In this paper, we present a comprehensive experimental and theoretical investigation on the decay of responsivity with increasing bias in a specific GaN Schottky PD. Photo-generated currents under different bias with varying load resistance were collected by a model SR830 DSP lock-in amplifier from a test circuit, and the dynamic parallel resistances of the devices are calculated as a differential curve from I–V characteristics measured by a Keithley 6430 source meter. The results reveal that the load resistance in the test circuit not only affects the static work point of the device, but also significantly influences the output responsivity of GaN Schottky detectors with low dynamic parallel resistance. In

[1] Author to whom any correspondence should be addressed.

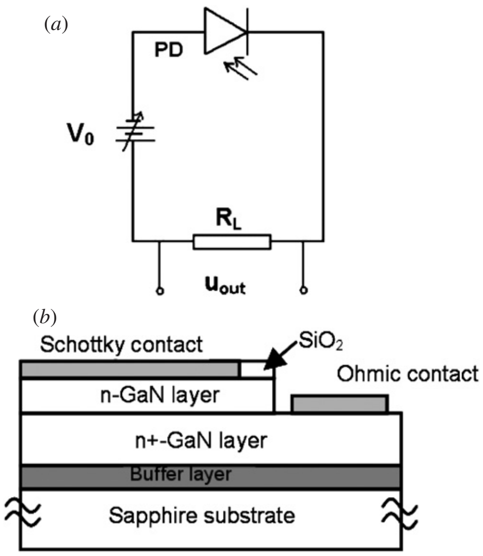

Figure 1. Schematic diagram of the test circuit (*a*) and the device structure (*b*).

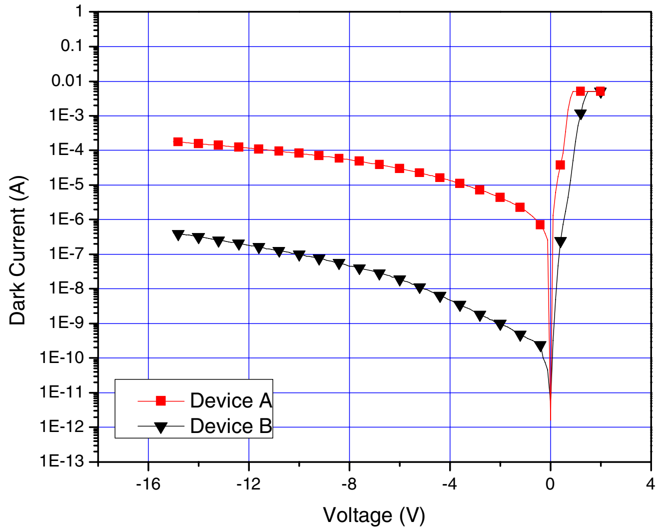

Figure 2. Dark current of devices A and B.

fact, an improper choice of load resistance would result in an unexpected reduction of the measured responsivity of devices, which is proved to originate from dynamic parallel resistance. This influence should be taken into account in the design of the ROIC.

We also provide a quantitative method by means of small signal analysis of the test circuit to determine the effect of load resistance and help establish load resistance in the circuit design to avoid responsivity decay.

2. Fabrication and experiment

The epilayer structure of the Schottky PDs was deposited on a *c*-plane sapphire substrate using metalorganic chemical vapour deposition (MOCVD). It contained a 4 μm thick heavily doped n^+-GaN, followed by a 0.4 μm unintentionally doped GaN active layer. Prior to the two layers mentioned above, an LT GaN buffer layer was deposited at 500 °C. The samples were measured by XRD, and a typical value of the full width at half maximum (FWHM) of a (0 0 0 2) rocking curve was 255 arcsec, indicating a comparatively low density of dislocations. From Hall measurements, the room temperature carrier densities of the GaN active layer and the heavily doped n^+-GaN layer were 1.6×10^{16} cm^{-3} and 3×10^{18} cm^{-3}, respectively.

Vertical Schottky barrier UV photodiodes were fabricated with a mesa structure. 1×1 mm^2 mesas were defined using reactive ion etching (RIE). A 350 nm SiO_2 passivation layer was grown by plasma-enhanced chemical vapour deposition (PECVD) and then etched in a BOE solution in order to expose the contact regions. Then Schottky contacts were formed on top of the mesas with semitransparent Ni/Au (5 nm/5 nm) films deposited by e-beam evaporation and annealed at 500 °C for 5 min. On the n^+-GaN layer, ohmic contacts were formed with e-beam evaporated Ti/Al/Ti/Au (15 nm/250 nm/50 nm/150 nm). The structure of the devices is shown in figure 1(*b*). After fabrication, the *I–V* characteristics and spectral responsivity of two typical devices A and B were measured. The devices were made from two chips with the same growth condition and material structure, whose XRD results are at the same order of magnitude. The system used to measure the responsivity consists of a xenon arc lamp as a light source, a monochromator, a chopper, a lock-in amplifier and a test circuit. In the test circuit, a tunable dc voltage source V_0 was connected to the tested detector and a load resistance R_L in series, as shown in figure 1(*a*).

During the experiment, the light radiated from the xenon lamp through a chopper was monochromatized and focused on the detector. The output photocurrent generated by the detector was extracted from the two ends of the load resistance using a lock-in amplifier and then calibrated with a Si PD. In this way, responsivities at different reverse bias voltages ranging from 0 V to 15 V were measured with different load resistances.

3. Results and discussion

Although sharing the same fabrication processing, the dark currents of the two devices are extraordinarily different from each other, as shown in figure 2.

The dark current at −5 V of device A is larger than that of device B by two orders of magnitude. This probably resulted from the different densities of point defects induced in these two chips during growth.

The measured responsivities of devices A and B with a relatively large load resistance (98.2 kΩ) at different reverse bias voltages (V_B) are shown in figure 3, and the maximum responsivity at a wavelength of 358 nm varying with V_B is shown in the inset of the same figure. The corresponding maximum of the photo-generated current is $\sim 5 \times 10^{-7}$ A and the photo-generated voltage is ∼50 mV. It reveals an unexpected decrease of responsivity with increasing V_B above 5 V in device A, while general increasing responsivity with rising V_B in device B. Theoretically, the responsivity of a

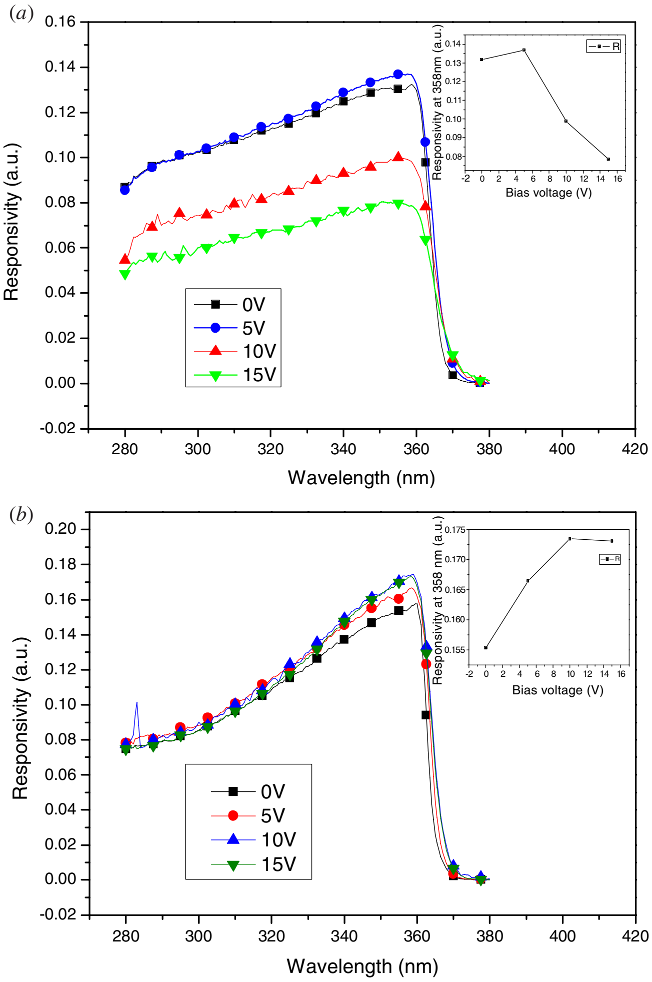

Figure 3. The measured responsivity of devices A (*a*) and B (*b*) with a load resistance of 98.2 kΩ at different reverse bias voltages.

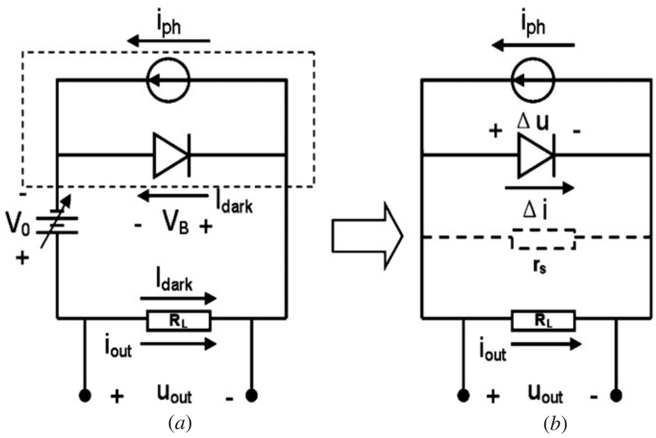

Figure 4. Equivalent transforms of the test circuit: (*a*) both dc and ac parts of the circuit; (*b*) ac part only.

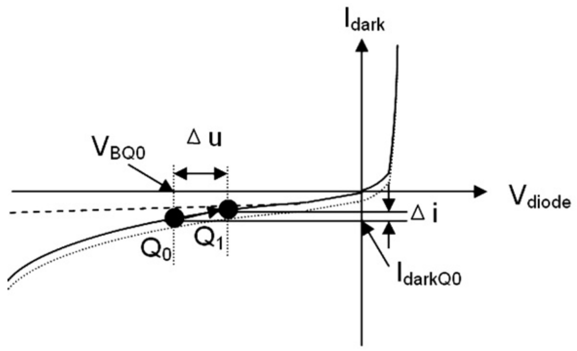

Figure 5. *I–V* curve schematic diagram of the Schottky photodetector. The broken line represents the ideal *I–V* characteristic while the solid line represents the non-ideal *I–V* curve, and the dotted line represents a sketch map of the illuminated *I–V* curve.

Schottky detector should increase a little with rising V_B and get saturated at a certain voltage, because the depletion region broadens with increasing V_B enhancing the electric field. Hence, the efficiency of collecting photo-generated carriers is improved [13]. But in our experiment with GaN Schottky UV detectors, it is observed that the responsivity may decrease with increasing V_B.

In order to explain this unexpected decrease, an equivalent transform of the tested detectors is employed. In an ideal PD, the photocurrent generated from the photodiode is determinate if incident light power remains constant. Accordingly, an ideal current source in parallel with a diode can be used as an equivalent transform of the PD [14], as shown in figure 4(*a*), where i_{ph} is the photocurrent generated by the PD, I_{dark} is the dark current flowing through the photodiode at bias V_B, R_L is the load resistance, i_{out} is the output current and u_{out} is the output voltage which is extracted using the lock-in amplifier.

The ac equivalent circuit extracted from the equivalent circuit is shown in figure 4(*b*). In the ac equivalent circuit, Δu is the variation of voltage drop through the diode. It originates from the photo-generated electromotive force due to the photovoltaic effect [14], whose direction is opposite to the built-in electric field. Δu supports the voltage drop u_{out} on R_L when i_{out} flows through R_L.

With a non-ideal Schottky PD, reverse current increases with bias voltage through a certain leakage channel. Considering such a device performing at work point Q_0 on the dark *I–V* curve as a solid line in figure 5, once the diode is illuminated, voltage varies (Δu) and the work point changes to Q_1 approximately along the *I–V* curve. Consequently, the current flowing through the diode changes (Δi), as shown in figure 5, which leads to an extra shunting channel in the circuit, making i_{out} lower than i_{ph}. While considering an ideal Schottky PD, since the reverse current gets saturated with rising V_B, the variation in the reverse bias voltage would not lead to any variation in the current flowing through the diode, as illustrated by a broken line in figure 5. In other words, Δi does not exist, so the output signal i_{out} is entirely equal to the photo-generated current i_{ph}. Ultimately, it is Δi that divides current from the photo-generated current i_{ph} and reduces the output signal i_{out}.

Quantitative analysis introduces the ratio $\Delta u/\Delta i$. Since the variation Δu is small enough, the ratio can be represented approximately as the differential of the dark *I–V* curve at point

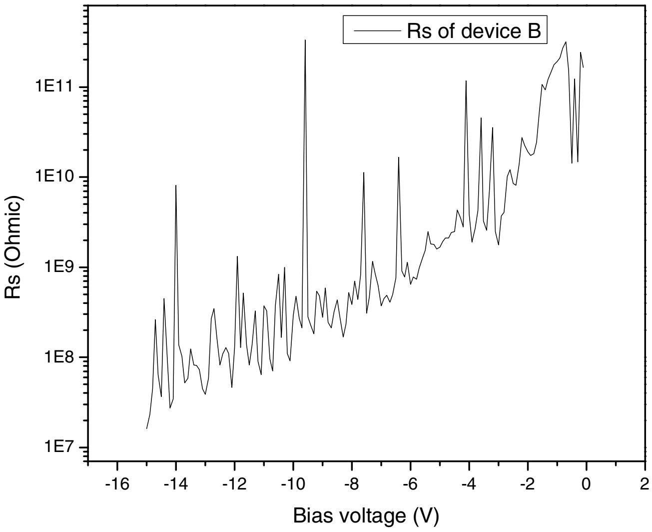

Figure 6. Approximate range of dynamic parallel resistance at different bias voltages of device B obtained by a derivative of the dark current *I*–*V* curve.

Q_0, which is known as the dynamic parallel resistance of the device and can be expressed as follows:

$$r_s = \frac{\Delta u}{\Delta i} = \frac{1}{f'(V_{\text{diod}})|_{V_{\text{diod}}=V_{BQ0}}}. \tag{1}$$

So the approximate distribution range of the dynamic parallel resistance of devices with different bias voltages can be extracted from the dark *I*–*V* characteristic as a differential curve. This resistance can be considered as parallel with an ideal photodiode and separates photocurrent from the output signal, as shown as r_s in figure 4(*a*). It may result from leakage tunnels whose amount varies at different bias voltages.

According to the equivalent circuit shown in figure 4(*b*), i_{out} can be expressed as follows:

$$i_{\text{out}} = i_{\text{ph}} - \Delta i, \tag{2}$$

and Δu can be expressed as follows:

$$\Delta u = u_{\text{out}} = i_{\text{out}} \times R_L = (i_{\text{ph}} - \Delta i) \times R_L. \tag{3}$$

From equations (1) and (3), equation (4) can be deduced:

$$\Delta u = (i_{\text{ph}} - \Delta i) \times R_L = \Delta i \times r_s. \tag{4}$$

According to the above equations, the relationship between the output signal i_{out} and the ideal photocurrent i_{ph} can be obtained as follows:

$$\begin{aligned} \Delta i &= \frac{R_L}{r_s + R_L} i_{\text{ph}} \\ i_{\text{out}} = i_{\text{ph}} - \Delta i &= \frac{r_s}{r_s + R_L} i_{\text{ph}} \\ &= \left[1 \Big/ \left(1 + \frac{R_L}{r_s}\right)\right] \times i_{\text{ph}}. \end{aligned} \tag{5}$$

According to equation (5), whether i_{out} approaches the actual photo-generated current i_{ph} depends on the factor $1\big/\left(1 + \frac{R_L}{r_s}\right)$. Consequently, all the devices operate as one of the two typical kinds of situations decided by the dynamic parallel resistance r_s.

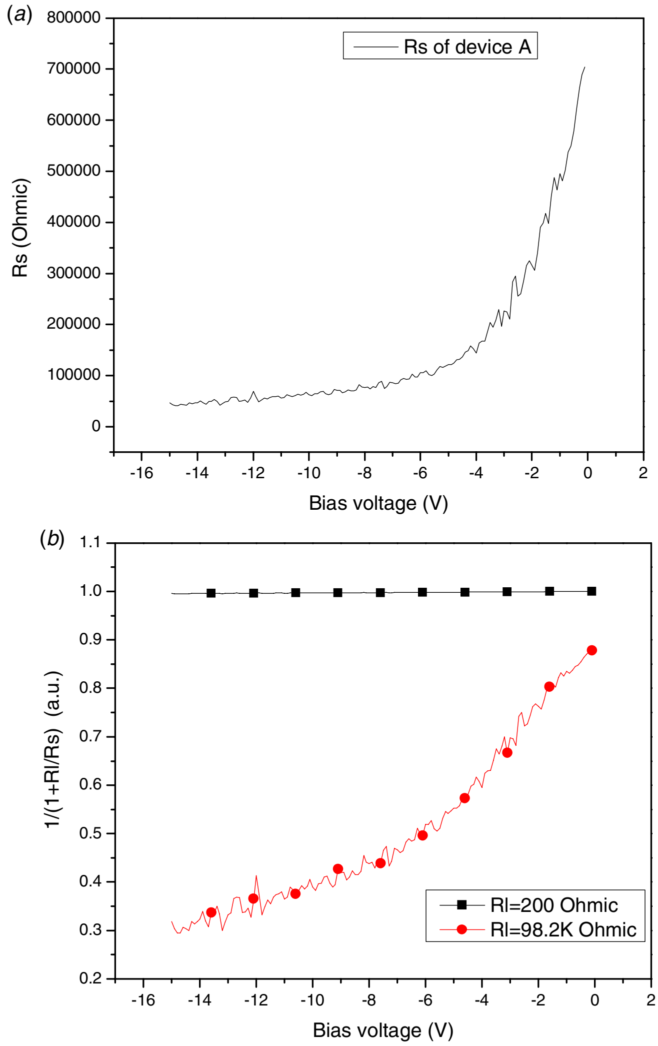

Figure 7. (*a*) The dynamic parallel resistance of device A and (*b*) the coefficient $1/(1 + \frac{R_L}{r_s})$ of device A with two different R_L: 200 Ω and 98.2 kΩ.

In the situation where the device presents a dynamic parallel resistance large enough compared to R_L, making the ratio R_L/r_s tend to zero, the factor $1\big/\left(1 + \frac{R_L}{r_s}\right)$ can be considered as constant 1 and does not relate to r_s or R_L. According to equation (5), i_{out} is always approximately equal to i_{ph} under this condition. In our experiment, device B performs in this situation. As shown in figure 6, the enormous dynamic parallel resistance of device B is larger than 10 MΩ, allowing the adoption of a load resistance as large as 98 kΩ, without inducing any responsivity decay, as shown in figure 3(*b*).

In the other situation, the dynamic parallel resistance of a device is as small as of the same order of magnitude as R_L, which results in a factor $1/(1 + \frac{R_L}{r_s})$ dependent on r_s. Since r_s changes with increasing bias voltage, i_{out} varies with bias and is no longer equal to i_{ph}. Device A is an example operating in this situation, whose dynamic parallel resistance is smaller than 100 kΩ in a large range of bias voltages, as shown in figure 7(*a*). The coefficient $1\big/\left(1 + \frac{R_L}{r_s}\right)$ of device A with different R_L is calculated and shown in figure 7(*b*). If a large load resistance (98 kΩ) is used, the coefficient $1\big/\left(1 + \frac{R_L}{r_s}\right)$ turns out to be small and decreases with increasing bias

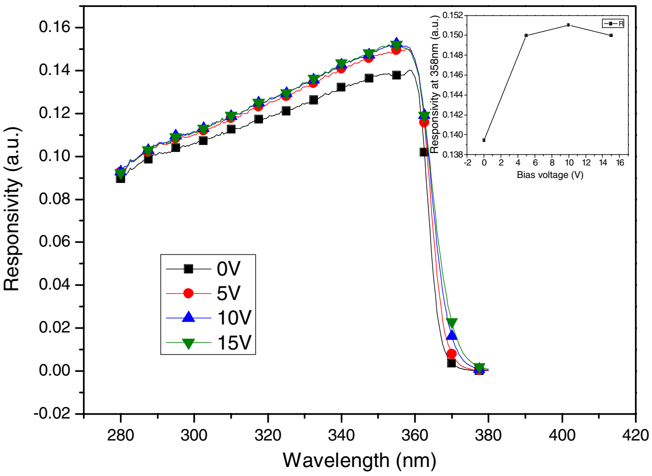

Figure 8. The responsivity of device A with a load resistance of 200 Ω at different reverse bias voltages.

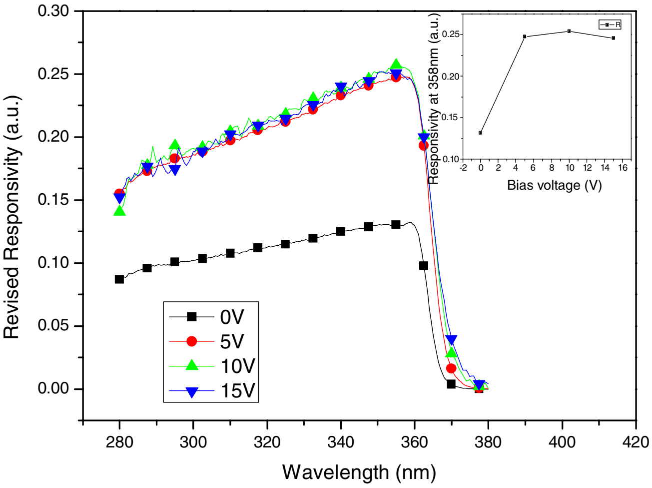

Figure 9. The substantial responsivity of device A at different bias voltages revised by $1/(1+\frac{R_L}{r_s})$.

voltage, indicating that the output signal would drop off with it, as shown in figure 3. To avoid this decrease, R_L should be much smaller than r_s to produce a low ratio R_L/r_s, making the coefficient $1\big/\left(1+\frac{R_L}{r_s}\right)$ again approach 1, as shown in figure 7(*b*). As a result, the responsivity of device A does not decay and follows the general variation trends, as shown in figure 8.

In addition, revised by the coefficient $1\big/\left(1+\frac{R_L}{r_s}\right)$, the substantial photo-generated current i_{ph} of device A with a large load resistance (98.2 kΩ) can be calculated from equation (5), and substantial responsivity is also achieved, as shown in figure 9. It recovers to the general situation of device B, as shown in the inset of figure 9, except for a little excursion caused by noises accumulated during calculations.

Basically, dynamic parallel resistance represents the dependence of leakage variation on reverse bias voltage, which is probably related to the conductive characteristic of leakage channels. Consequently, the difference between dynamic parallel resistances of devices A and B may originate from different kinds of leakage channel dominating in these devices.

The calculation results of the measurement data provide a good proof for previous analysis and inference, making a complete explanation of the phenomenon that measured responsivity decays with increasing bias voltage. It is shown that for devices with enormous dynamic parallel resistance, the choice of load resistance can change unlimitedly in a large range. However, devices with a low dynamic parallel resistance need load resistance as small as possible; otherwise the measured responsivity may decay with increasing reverse bias voltage. With these demonstrations, it is suggested that the choice of load resistance should be made carefully in the design of the read-out circuit of FPA according to the device's dynamic parallel resistance, in order to avoid an undesired decrease in measured responsivity and obtain fine performance of the photodetecting system.

4. Conclusion

According to the experiment and analysis described above, it is concluded that the measured responsivity of GaN Schottky photodetectors is related to their dynamic parallel resistance and the load resistance used in the circuit. Devices with a low dynamic parallel resistance need load resistance as small as possible, so that the measured photocurrent can approach the substantial photocurrent generated in the device. On the other hand, for devices with enormous dynamic parallel resistance, the choice of load resistance is more unrestricted. This result is referential in design of photodetector read-out circuits, indicating that the input resistance of read-out circuits should be designed carefully according to the *I–V* characteristic of the photodetectors to avoid the responsivity decay at reverse bias voltage.

Acknowledgment

The authors acknowledge the support from the National Natural Science Foundation of China (grant nos 60776047, 60506001, 60476021 and 60576003).

References

[1] Morkoc H, Di Carlo A and Cingolani R 2002 *Solid-State Electron.* **46** 157
[2] Monroy E, Calle F, Pau J L, Sánchez F J and Muñoz E 2000 *J. Appl. Phys.* **88** 4
[3] Khan M A, Kuznia J N, Olason D T, Van Hove J M, Blasingame M and Reitz L F 1992 *Appl. Phys. Lett.* **60** 2917
[4] Monroy E, Munoz E, Sanchez F J, Calle F, Calleja E, Beaumout B, Gibart P, Munoz J A and Cusso F 1998 *Semicond. Sci. Technol.* **13** 1042
[5] Parish G, Keller S, Kozodoy P, Ibbetson J A, Marchand H, Fini P T, Fleischer S B, DenBaars S P and Mishra U K 1999 *Appl. Phys. Lett.* **75** 247
[6] Monroy E, Hamilton M, Walker D, Kung P, Sanchez F J and Razeghi M 1999 *Appl. Phys. Lett.* **74** 1171
[7] Chen Q, Yang J W, Osinsky A, Gangopadhyay S, Lim B, Anwar M Z, Asif Khan M, Kuksenkov D and Temkin H 1997 *Appl. Phys. Lett.* **70** 2277
[8] Huang Z C, Chen J C and Wickenden D 1997 *J. Cryst. Growth* **170** 362

[9] Chen C H, Chang S J, Su Y K, Chi G C, Chi J Y, Chang C A, Sheu J K and Chen J F 2001 *IEEE Photonics Technol. Lett.* **13** 848

[10] Walker D, Monroy E, Kung P, Wu J, Hamilton M, Sanchez F J, Diaz J and Razeghi M 1999 *Appl. Phys. Lett.* **74** 762

[11] McClintock R, Mayes K, Yasan A, Shiell D, Kung P and Razeghi M 2005 *Appl. Phys. Lett.* **86** 011117

[12] Kuryatkov V V, Borisov B A and Nikishin S A 2006 *J. Appl. Phys.* **100** 096104

[13] Yuan G P and Yang F 2006 *Photoelectric Detection Technology and Application* (Beihang: Publishing House of Beihang University) pp 37, 71–109 (in Chinese)

[14] Gu Z Y, Tian L and Fu L 1995 *Semiconductor Physics* (China: Publishing House of Electronics Industry) p 312 (in Chinese)